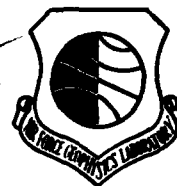


ADA082458

AFGL-TR-79-0277
AIR FORCE SURVEYS IN GEOPHYSICS, NO. 418 ✓

12
✓
TEL



Seismic Hazards Estimation Study for Vandenberg AFB

JAMES C. BATTIS

14 November 1979

DTIC
SELECTED
APR 1 1980
A

Approved for public release; distribution unlimited.

TERRESTRIAL SCIENCES DIVISION PROJECT 7600
AIR FORCE GEOPHYSICS LABORATORY
HANSOM AFB, MASSACHUSETTS 01731

AIR FORCE SYSTEMS COMMAND, USAF



DDC FILE COPY

80

3

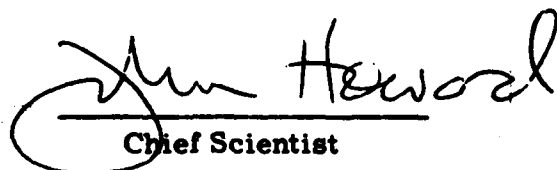
22

061

This report has been reviewed by the ESD Information Office (OI) and is releasable to the National Technical Information Service (NTIS).

This technical report has been reviewed and is approved for publication.

FOR THE COMMANDER


Chief Scientist

Qualified requestors may obtain additional copies from the Defense Documentation Center. All others should apply to the National Technical Information Service.

Unclassified

SECURITY CLASSIFICATION OF THIS PAGE (When Data Entered)

| REPORT DOCUMENTATION PAGE | | READ INSTRUCTIONS BEFORE COMPLETING FORM |
|--|----------------------------------|--|
| 1. REPORT NUMBER | 2. GOVT ACCESSION NO. | 3. RECIPIENT'S CATALOG NUMBER |
| 14 AFGL-TR-79-0277 | AFGL-AFSG-428 | |
| 4. TITLE (and Subtitle) | | 5. TYPE OF REPORT & PERIOD COVERED |
| 6 SEISMIC HAZARDS ESTIMATION STUDY FOR VANDENBERG AFB | | Scientific. Interim. |
| 7. AUTHOR(s) | 6. PERFORMING ORG. REPORT NUMBER | |
| 10 James C. Battis | AFSG No. 418 | |
| 9. PERFORMING ORGANIZATION NAME AND ADDRESS | | 8. CONTRACT OR GRANT NUMBER(s) |
| Air Force Geophysics Laboratory (LWH) Hanscom AFB Massachusetts 01731 | | 12 35 |
| 11. CONTROLLING OFFICE NAME AND ADDRESS | | 10. PROGRAM ELEMENT, PROJECT, TASK AREA & WORK UNIT NUMBERS |
| Air Force Geophysics Laboratory (LWH) Hanscom AFB Massachusetts 01731 | | 16 62101F 76000902 |
| 14. MONITORING AGENCY NAME & ADDRESS (if different from Controlling Office) | | 17. REPORT DATE |
| | | 11 14 Nov 79 |
| | | 18. NUMBER OF PAGES |
| | | 32 |
| | | 15. SECURITY CLASS. (of this report) |
| | | Unclassified |
| | | 15a. DECLASSIFICATION/DOWNGRADING SCHEDULE |
| 16. DISTRIBUTION STATEMENT (of this Report) | | |
| Approved for public release; distribution unlimited. | | |
| 17. DISTRIBUTION STATEMENT (of the abstract entered in Block 20, if different from Report) | | |
| 9 Air Force surveys in geophysics | | |
| 18. SUPPLEMENTARY NOTES | | |
| 19. KEY WORDS (Continue on reverse side if necessary and identify by block number) | | |
| Seismic risk Earthquake effects Seismic motions Seismicity | | |
| 20. ABSTRACT (Continue on reverse side if necessary and identify by block number) | | |
| The seismic hazard at Vandenberg AFB was investigated using both statistical analysis of the temporal and spatial distribution of historic earthquake activity within 500 km of Point Arguello, California, and deterministic methods based on knowledge of earthquake faults and recency of faulting near the installation. The results of these studies included probabilistic estimates of peak ground motions and maximum credible ground motions at Vandenberg AFB. This information was used to generate horizontal design response spectra which are more directly applicable for the analysis of the behavior of engineering | | |

DD FORM 1 JAN 73 1473 EDITION OF 1 NOV 65 IS OBSOLETE

Unclassified

SECURITY CLASSIFICATION OF THIS PAGE (When Data Entered)

409578

alt

Unclassified

SECURITY CLASSIFICATION OF THIS PAGE(When Data Entered)

20. (Cont)

structures to earthquake induced motions.

Unclassified

SECURITY CLASSIFICATION OF THIS PAGE(When Data Entered)

Contents

| | |
|--|----|
| 1. INTRODUCTION | 5 |
| 2. REGIONAL GEOLOGY | 6 |
| 3. STATISTICAL HAZARD ANALYSIS | 8 |
| 3.1 Seismic Risk Method | 8 |
| 3.2 Regional Seismicity Study | 8 |
| 3.3 Ground Motion Attenuation | 10 |
| 3.4 Seismic Risk Estimation | 13 |
| 3.5 Composite Design Response Spectra | 18 |
| 4. NON-STATISTICAL HAZARD ANALYSIS | 21 |
| 4.1 Geologic Methods | 21 |
| 4.2 Quaternary Faulting Near Vandenberg AFB | 21 |
| 4.3 Maximum Credible Earthquakes | 23 |
| 4.4 Maximum Credible Ground Motions | 23 |
| 4.5 Maximum Credible Design Response Spectra | 25 |
| 5. LOCAL EARTHQUAKE HISTORY | 27 |
| 6. CONCLUSIONS | 30 |
| REFERENCES | 31 |

Illustrations

| | |
|---|----|
| 1. Generalized Geologic Map of Western Santa Barbara County, California | 7 |
| 2. Source Regions Used in the Vandenberg AFB Hazard Study | 9 |
| 3. Ground Motion Attenuation Functions | 12 |
| 4. Annual Seismic Risk Curves for Vandenberg AFB | 14 |
| 5. Twenty-year Lifetime Seismic Risk Curves for Vandenberg AFB | 15 |
| 6. Composite Horizontal Design Response Spectra for Vandenberg AFB Using 10 (a), 100 (b), and 1000 (c) Year Return Period Ground Motions | 19 |
| 7. Twenty-year Lifetime Composite Horizontal Response Spectra for Vandenberg AFB Using Ground Motions With Risks of 0.9 (a), 0.1 (b), and 0.01 (cc) | 20 |
| 8. All Faults Within 50 km and Faults With Quaternary Displacements Within 100 km of Point Arguello | 22 |
| 9. Maximum Credible Ground Motions in Western Santa Barbara County at the 90% Confidence Level; (a) Acceleration in %g; (b) Velocity in cm/sec; (c) Displacement in cm | 25 |
| 10. Maximum Credible Horizontal Design Response Spectra for: (a) Point Sal; (b) Point Arguello for an Earthquake on the Hosgri Fault Zone; (c) Point Arguello for an Earthquake on the San Andreas Fault Zone | 26 |
| 11. Earthquake Epicenters, Western Santa Barbara County, California | 28 |
| 12. Cumulative Recurrence Curve for the Coastal Faults Source Region | 29 |
| 13. Epicenter Determinations for the 1927 Lompog Earthquake With Rossi-Forel Iseismal Contours (After Hanks, 1979) | 29 |

Tables

| | |
|---|----|
| 1. California-Nevada Source Region Parameters | 10 |
| 2. Peak Ground Motion Attenuation Functions (After McGuire, 1974) | 11 |
| 3. Peak Ground Motion Annual Risk Levels for Vandenberg AFB | 15 |
| 4. Peak Ground Motion Risk Levels for a 20-Year Lifetime at Vandenberg AFB | 15 |
| 5. Modified Mercalli Intensity Scale of 1931 | 17 |
| 6. Annual Risk Equivalent Intensities at Vandenberg AFB | 18 |
| 7. Horizontal Design Response Spectra Amplification Factors at Control Point Frequencies | 21 |
| 8. Major Faults Near Vandenberg AFB and Associated Maximum Credible Earthquakes | 24 |
| 9. Maximum Credible Ground Motions at Point Sal and Point Arguello (90% confidence level) | 24 |

Seismic Hazards Estimation Study for Vandenberg AFB

1. INTRODUCTION

The Terrestrial Sciences Division of the Air Force Geophysics Laboratory, in support of both the Space Transporter System (STS) and the M-X missile program, has conducted an evaluation of the seismic hazard at Vandenberg AFB. This installation, located in coastal south-central California, is situated in one of the more seismically active regions of the United States and is characterized by a number of fault systems capable of generating major earthquakes. To accomplish the objectives of this study, the seismic hazard at Vandenberg AFB was investigated using both statistical analysis of the temporal and spatial distribution of historic earthquake activity within 500 km of Point Arguello, California, and deterministic methods based on knowledge of earthquake faults and recency of faulting near the installation. The results of these studies include probabilistic estimates of peak ground motions and maximum credible ground motions at Vandenberg AFB. This information was used to generate horizontal design response spectra that are more directly applicable for the analysis of the behavior of engineering structures to earthquake induced motions.

(Received for publication 9 November 1979)

2. REGIONAL GEOLOGY

Vandenberg AFB is located in coastal south-central California in an area forming the boundary between two physiographic regions. The southern end of the facility, including Point Arguello, lies within the Transverse Ranges Province while the northern part of the facility is in the Coastal Ranges.¹ The border between these two regions runs approximately along the northern edge of the Santa Ynez Mountains on a general east-west trend north of Honda² along the Santa Ynez River Fault (see Figure 1). The tectonic and geologic history of the area is dominated by the effects of the overriding of the ancestral East Pacific Rise by the North American Plate during the Late Cenozoic.

The Coastal Ranges are thought to have resulted from the collision of the North American Plate and a microcontinent during the Late Jurassic as the North American Plate overrode an ancestral rise-trench system located off the Pacific Coast.³ This collision produced a westward protruding bulge in the continental margin which included most of the land west of the Rinconada Fault and north of Point Arguello (Figure 1). From the Late Jurassic to mid-Cenozoic a new rise-trench system developed⁴ and was again overridden at approximately 30 m.y. B.P.⁵ Two ridge-fault-trench triple junctions formed offshore of Southern California at the intersection point between the ancestral East Pacific Rise and the trench system. The Mendocino triple junction moved to the north while the Rivera migrated southward.

It is thought that between 18 and 8 m.y. B.P., instabilities associated with the Rivera triple junction generated rifting along the Baja Pacific coast with northerly translation of the rifted block along a ridge-trench transform fault. Resistance to this motion was provided by the bulge of the Coastal Ranges and resulted in the rotation and compression of the northern tip of the rifted crust and development of the Transverse Ranges.¹

1. Crouch, J. (1979) Neogene tectonic evolution of the California continental borderland and western transverse ranges, Geol. Soc. Am. Bull. 90:338-345.
2. Sylvester, A., and Darrow, A. (1979) Structure and neotectonics of the Western Santa Ynez fault system in Southern California, Tectonophysics 52:389-405.
3. Hsü, K. (1971) Franciscan melanges as a model for eugeosynclinal sedimentation and underthrusting tectonics, J. Geophys. Res. 76:1162-1170.
4. Atwater, T. (1970) Implications of plate tectonics for the Cenozoic tectonic evolution of Western North America, Geol. Soc. Am. Bull. 81:3515-3536.
5. Johnson, J., and Normark, W. (1974) Neogene tectonic evolution of the Salinian block, West-Central California, Geology 2:11-14.

Since the overriding of the rise system, the dominant tectonic force in coastal California has been the right lateral horizontal shear between the Pacific and North American Plate. The San Andreas Fault system is the main feature on which the accumulated strain is released. Additional and significant motion is absorbed along the other northwest trending faults of the region and internally by folding. Within the Transverse Ranges, the primary mechanism is thrust faulting with left lateral motion, indicating the difference in tectonic activity between it and the Coastal Ranges Province.

3. STATISTICAL HAZARD ANALYSIS

3.1 Seismic Risk Method

As the first step in the seismic hazards analysis, a statistical study based on the historic earthquake catalogue was initiated. In this procedure, a regional seismicity study is used to identify the zones of seismic activity that could effect the level of risk at the site of interest. Estimations, in an historic average sense, of the levels of activity within each source region are made. The derived spatial and temporal characterization of earthquake occurrence can then be combined with empirical ground motion attenuation functions to generate statistical estimates for seismic hazard at the site of interest.

3.2 Regional Seismicity Study

The necessary seismicity studies required for analysis of the seismic risk at Vandenberg AFB have been previously conducted in conjunction with risk studies for other sites in the western United States.⁶ As a data base for these studies the National Oceanic and Atmospheric Administration Earthquake Data File⁷ was utilized. On the basis of the earthquake epicenters reported on this file, eleven significant source regions were identified within a radius of 500 km of Vandenberg AFB (Figure 2). These source regions were defined on the basis of clustering of epicenters and tectonic setting. Due to the various inaccuracies of the statistical risk method, it was not deemed necessary nor desirable to attempt to model seismic features on a finer scale.

6. Battis, J. (1978b) Geophysical Studies for Missile Basing: Seismic Risk Studies in the Western United States, Texas Instruments Inc., Final Scientific Report, ALEX(02)-FSR-78-01.

7. Meyers, H., and von Hake, C. (1976) Earthquake Data File Summary, National Geophysical and Solar-Terrestrial Data Center Report KGRD-5.

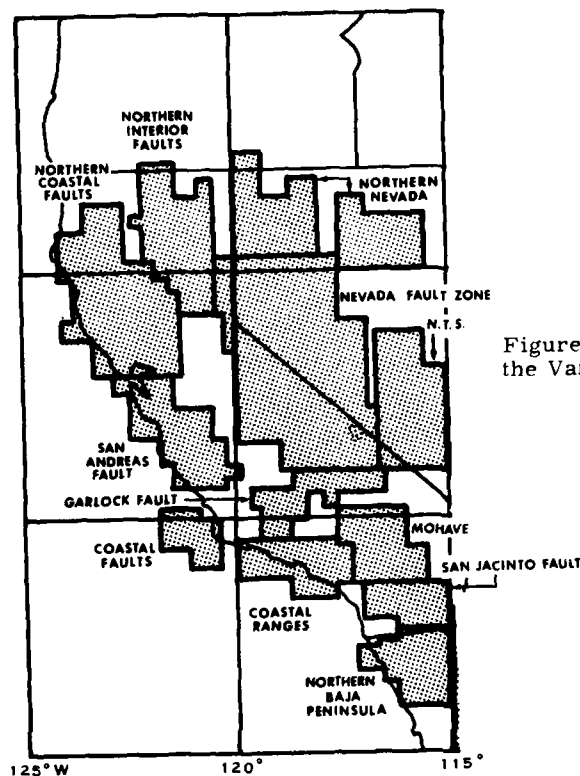


Figure 2. Source Regions Used in the Vandenberg AFB Hazard Study

For each of the defined source regions, estimates of the level of seismic activity were made by fitting to the source region data the standard recurrence function⁸

$$\text{Log}_{10} (N) = A - bM_L \quad (1)$$

where

N = number of events per year of local magnitude, M_L , or greater and,

A and b = regression parameters.

The results of this analysis for each source region are given in Table 1 along with estimates of the maximum magnitude earthquake and the area of each source.

8. Richter, C. (1958) Elementary Seismology, W. H. Freeman and Co., San Francisco, CA.

The maximum magnitude earthquake was generated either by adding $0.5 M_L$ to the largest magnitude event recorded in the source region or by calculation of the maximum credible earthquake based on known fault lengths in the source region.^{9, 10}

Table 1. California-Nevada Source Region Parameters

| Source | Area | A_{M_L} | b_{M_L} | M_L^{\max} |
|-------------------------|--------------------|-----------|-----------|--------------|
| Coastal Ranges | 2.44×10^4 | 5.226 | 1.0382 | 6.1 |
| Coastal Faults | 9.61×10^3 | 3.8053 | 0.9086 | 6.5 |
| Northern Baja Peninsula | 2.86×10^4 | 4.7971 | 0.8838 | 6.9 |
| San Jacinto | 1.77×10^4 | 4.7061 | 0.9079 | 6.5 |
| Mojave | 2.24×10^4 | 4.9528 | 1.0242 | 6.5 |
| San Andreas | 3.66×10^4 | 4.1992 | 0.8436 | 7.5 |
| Northern Coastal | 6.08×10^4 | 4.2143 | 0.9492 | 7.25 |
| Northern Interior | 3.38×10^4 | 4.4167 | 1.1746 | 7.0 |
| Nevada Fault Zone | 1.36×10^5 | 4.2192 | 0.7580 | 8.25 |
| Garlock Fault | 1.95×10^4 | 4.7402 | 0.9328 | 7.75 |
| Nevada Test Site | 3.91×10^4 | 4.3264 | 0.7490 | 7.0 |

3.3 Ground Motion Attenuation

To carry out the statistical hazard evaluation it is necessary not only to know the distribution of earthquake activity but also to be able to predict the ground motions induced by the activity at some remote site. Various empirical studies have been conducted to generate these ground motion attenuation functions.^{11, 12} Typically these equations take the form

$$g = a_1 e^{a_2 M_L} (R + a_3)^{-a_4} \quad (2)$$

9. Greensfelder, R. (1974) Maximum Credible Rock Acceleration From Earthquakes in California, California Division of Mines and Geology, Map Sheet 25.
10. Battis, J. (1978a) Geophysical Studies for Missile Basing Seismic Risk Studies in the Western United States, Texas Instruments Inc., Scientific Report No. 2, ALEX(02)-ISR-78-01.
11. Esteva, L. (1970) Seismic risk and seismic design decisions, in Seismic Design for Nuclear Power Plants, R. Hansen, Editor, MIT Press, pp 142-182.
12. McGuire, R. (1974) Seismic Structural Response Risk Analysis Incorporating Peak Response Regressions on Earthquake Magnitude and Distance, M.I.T. Dept. of Civil Eng. Research Report R74-51.

where

g = ground motion level,

M_L = event local magnitude,

R = event to site distance,

$a_1, -a_4$ = regression parameters.

At best these equations are of only limited accuracy as they do not incorporate any radiation pattern or travel path modifications.

For the purposes of this analysis, the peak ground acceleration, velocity, and displacement equations determined by McGuire¹² were utilized. The regression parameters for these equations are given in Table 2. In Figures 3a to 3c the predicted attenuation curves for acceleration, velocity, and displacement over a range of magnitudes from 4 to 8 M_L are shown.

Table 2. Peak Ground Motion Attenuation Functions
(After McGuire, 1974)

| | a_1 | a_2 | a_3 | a_4 | $\ln a_1$ | σ^* |
|----------------------------------|-------|-------|-------|-------|-----------|------------|
| Acceleration (cm/s^2) | 472.0 | 0.645 | 25.0 | 1.30 | 6.16 | 0.511 |
| Velocity (cm/s) | 5.64 | 0.921 | 25.0 | 1.20 | 1.73 | 0.629 |
| Displacement (cm) | 0.393 | 0.99 | 25.0 | 0.88 | -0.934 | 0.76 |

* σ is for the Log_e of the ground motion parameter.

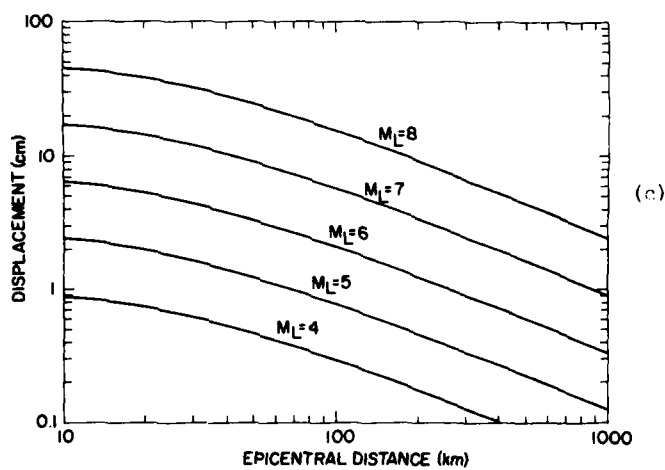
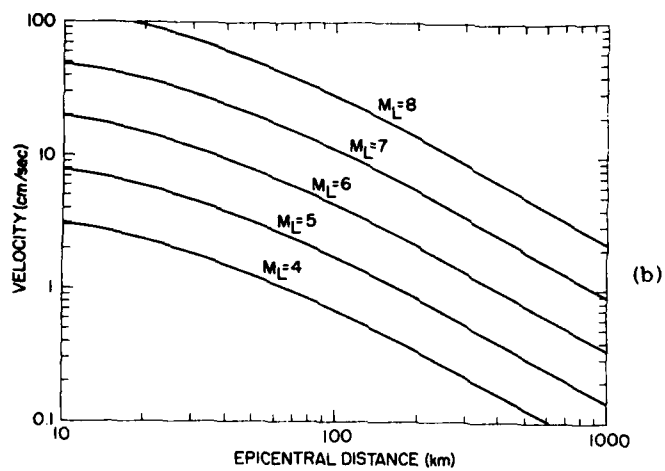
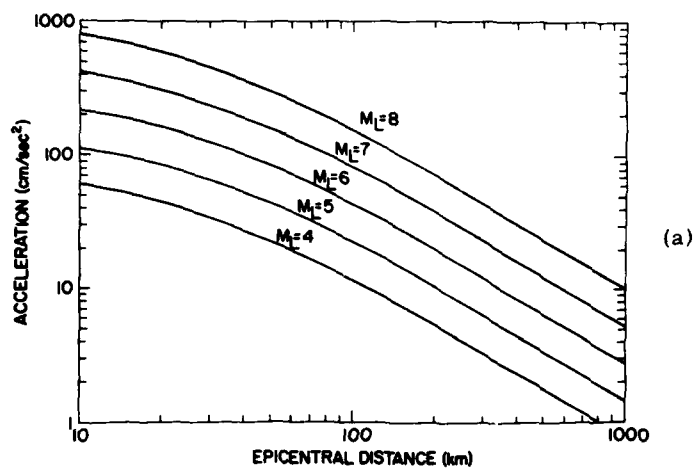


Figure 3. Ground Motion Attenuation Functions

3.4 Seismic Risk Estimation

Using a method proposed by Cornell¹³ and implemented in a FORTRAN computer program by McGuire¹⁴ the temporal and spatial distribution of seismic activity and the ground motion attenuation functions can be combined into a single statement of the probability of attaining a given level of ground motion at the site of interest. In this procedure, the probability that the ground motion level will reach or exceed a specified level, m_g , is defined as the integral of the product of the independent probability density functions for magnitude, f_S , distance, f_R , and the conditional probability of reaching or exceeding m_g given magnitude, s , and distance, r . This can be stated as an equation

$$P[M_g \geq m_g] = P[M_g \geq m_g | s \text{ and } r] f_S(s) f_R(r) ds dr \quad (3)$$

where

$P[M_g \geq m_g | s \text{ and } r]$ is the condition probability given event magnitude and distance.

The conditional probability of Eq. (3) is a function of the ground motion attenuation equation and its standard deviation. The function, $f_S(s)$ is derived from each source region recurrence curve while $f_R(r)$ incorporates the spatial relationship between source region and site of interest. Evaluation of the integral yields the probability of one event from the specified source region reaching or exceeding m_g . By multiplying this value by the expected number of events in the region and accumulating over all source areas, the total expected number of events meeting the condition, $E[M_g \geq m_g]$, is obtained. Assuming earthquake occurrence is a Poisson process, the annual risk is given by

$$R[M_g \geq m_g] = 1 - e^{-E[M_g \geq m_g]} \quad (4)$$

The statistical evaluation of the seismic hazard was carried out for three locations within Vandenberg AFB to assess the variation in seismic hazard across the facility. The sites selected for examination were Point Arguello, Vandenberg Village, and Point Sal. While a slight variation in peak ground acceleration risk levels was observed, the differences amounted to less than 3 percent in the

13. Cornell, C. (1968) Engineering seismic risk analysis, Bull. Seism. Soc. Am. 58:1503-1606.
14. McGuire, R. (1976) FORTRAN Computer Program for Seismic Risk Analysis, U.S. Geol. Surv. Open-File Report 76-67.

accelerations at a given risk level. Given the errors in the ground motion estimation process, the observed gradient is negligible. It is thought that the variations are more the effect of the proximity of the Coastal Faults source region boundaries, which are somewhat arbitrary, at this scale to the test locations (Figure 2), than to any valid physical cause.

As a result of this test and due to the location of Satellite Launch Complex 6 (SLC6), the Point Arguello site was used for all other risk calculations. The estimated seismic risk curves for peak ground acceleration, velocity, and displacement for this site are shown in Figure 4. Ground motion levels associated with specific levels of annual risk are given in Table 3. All calculations were made at the 90 percent confidence level. In addition, the risk levels were calculated for the expected 20-yr lifetime of SLC6. These risk curves are given in Figure 5 and selected points are tabulated in Table 4.

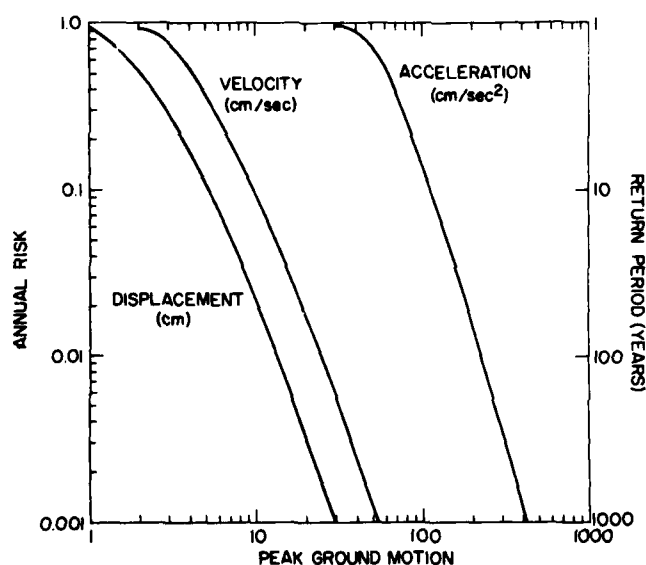


Figure 4. Annual Seismic Risk Curves for Vandenberg AFB

Table 3. Peak Ground Motion Annual Risk Levels for Vandenberg AFB

| Annual Risk | Return Period (Years) | Acceleration (cm/sec ²) | Velocity (cm/sec) | Displacement (cm) |
|-------------|-----------------------|-------------------------------------|-------------------|-------------------|
| 0.9 | 1.11 | 41.4 | 2.56 | 1.13 |
| 0.5 | 2 | 61.5 | 4.03 | 2.22 |
| 0.2 | 5 | 86.8 | 6.52 | 3.67 |
| 0.1 | 10 | 109.1 | 8.88 | 5.07 |
| 0.05 | 20 | 135.5 | 11.08 | 6.83 |
| 0.02 | 50 | 178.7 | 17.28 | 9.93 |
| 0.01 | 100 | 219.3 | 22.67 | 13.02 |
| 0.005 | 200 | 268.0 | 29.48 | 16.89 |
| 0.002 | 500 | 346.3 | 41.03 | 23.45 |
| 0.001 | 1000 | 417.2 | 52.00 | 29.68 |

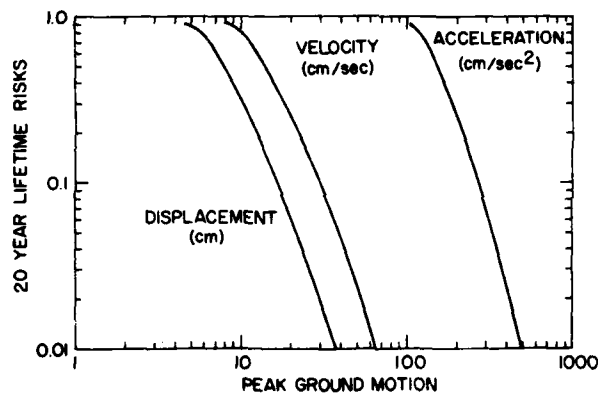


Figure 5. Twenty-Year Lifetime Seismic Risk Curves for Vandenberg AFB

Table 4. Peak Ground Motion Risk Levels for a 20-Year Lifetime at Vandenberg AFB

| Lifetime Risk | Return Period (20-Yr Periods) | Acceleration (cm/sec ²) | Velocity (cm/sec) | Displacement (cm) |
|---------------|-------------------------------|-------------------------------------|-------------------|-------------------|
| 0.9 | 1.11 | 106.2 | 8.35 | 4.88 |
| 0.5 | 2.0 | 152.2 | 13.86 | 7.97 |
| 0.2 | 5.0 | 212.9 | 21.75 | 12.53 |
| 0.1 | 10.0 | 264.1 | 28.92 | 16.56 |
| 0.05 | 20.0 | 323.3 | 37.57 | 21.50 |
| 0.02 | 50.0 | 416.2 | 51.79 | 29.57 |
| 0.01 | 100.0 | 498.1 | 65.05 | 37.10 |

At this point, the limitations of these estimates should be discussed. It is expected that the primary source of error in this study would be carried in the ground motion attenuation functions where the standard errors of the natural logarithm of the ground motions is 0.51 or greater. This error alone probably overwhelms all other sources. For example, the 100-yr return period acceleration of 219.3 cm/sec^2 at the 90 percent confidence level is equivalent to a 113 cm/sec^2 at the 50 percent confidence level or the mean expected value. In general, the assignment of activity levels to the source regions is considered satisfactory and not appreciably different from other studies.¹⁵

As Vandenberg AFB is located within one of the seismic source regions, an additional source of error, on a local scale, is introduced. In the risk analysis process, within a source region, the distribution of seismic activity is assumed to be random. In reality, the activity is typically concentrated along fault zones. As the highest accelerations are expected near the causative faults, the affect of the assumption is to reduce the apparent risk near the active faults and to increase the risk away from these faults. This is a local effect requiring additional geologic studies but which could be significant.

The correlation of peak ground motions with expected levels of damage is difficult without a detailed study of the foundation soil conditions and the engineering parameters of the structure of interest. Several studies have attempted to derive equations relating ground motion levels and site intensity.^{16, 17, 18} Typically, it is found that peak ground velocity correlates reasonably with intensity but acceleration and displacement are weakly correlated.

For the purpose of giving some limited physical meaning to the ground motions levels predicted for Vandenberg AFB the equations derived by Trifunac and Brady¹⁶ were used to convert ground motions for various levels of risk to intensity. These relationships are, for acceleration

$$\text{Log } a = 0.014 + 0.30 I, \quad (5)$$

15. Allen, C., St. Amond, P., Richter, C., and Nordquist, J. (1965) Relationship between seismicity and geological structure in the Southern California Region, Bull. Seism. Soc. Am. 55:753-797.
16. Trifunac, M., and Brady, A. (1975) On the correlation of seismic intensity scales with peaks of recorded strong ground motion, Bull. Seism. Soc. Am. 65:139-162.
17. McGuire, R. (1977) The use of intensity data in seismic-hazard analysis, Proc. Sixth World Conf. on Earthquake Engineering, pp 709-714.
18. Murphy, J., and O'Brien, L. (1977) The correlation of peak ground acceleration amplitude with seismic intensity and other physical parameters, Bull. Seism. Soc. Am. 67:877-915.

for velocity

$$\text{Log } v = -0.63 = 0.25 I \quad (6)$$

and for displacement

$$\text{Log } d = -0.53 = 0.19 I \quad (7)$$

where I is the correlated site intensity in terms of the Modified Mercalli Scale for average soil conditions. The descriptions used in assigning intensity are given in Table 5. Table 6 lists the predicted intensity based on the accelerations, velocities, and displacements given in Table 3 at specific annual risk levels for Vandenberg AFB. To demonstrate the low correlation of ground motion and intensity it is interesting to note that the equations developed by McGuire¹⁷ predict intensities similar to those given for acceleration using velocity and displacement as input data.

Table 5. Modified Mercalli Intensity Scale of 1931

| | |
|--|---|
| I. Not felt except by a very few under specially favorable circumstances. (I Rossi-Forel scale.) | by persons driving motorcars. (VIII Rossi-Forel scale.) |
| II. Felt only by a few persons at rest, especially on upper floors of buildings. Delicately suspended objects may swing. (I to II Rossi-Forel scale.) | VIII. Damage slight in specially designed structures; considerable in ordinary substantial buildings with partial collapse; great in poorly built structures. Panel walls thrown out of frame structures. Fall of chimneys, factory stacks, columns, monuments, walls. Heavy furniture overturned. Sand and mud ejected in small amounts. Changes in well water. Persons driving motorcars disturbed. (VIII+ to IX- Rossi-Forel scale.) |
| III. Felt quite noticeably indoors, especially on upper floors of buildings, but many people do not recognize it as an earthquake. Standing motorcars may rock slightly. Vibration like passing of truck. Duration estimates. (III Rossi-Forel scale.) | IX. Damage considerable in specially designed structures; well-designed frame structures thrown out of plumb; great in substantial buildings, with partial collapse. Buildings shifted off foundations. Ground cracked conspicuously. Underground pipes broken. (IX+ Rossi-Forel scale.) |
| IV. During the day felt indoors by many, outdoors by few. At night some awakened. Dishes, windows, doors disturbed; walls make creaking sound. Sensation like heavy truck striking building. Standing motorcars rocked noticeably. (IV to V Rossi-Forel scale.) | X. Some well-built wooden structures destroyed; most masonry and frame structures destroyed with foundations; ground badly cracked. Rails bent. Landslides considerable from riverbanks and steep slopes. Shifted sand and mud. Water splashed (slopped) over banks. (X Rossi-Forel scale.) |
| V. Felt by nearly everyone, many awakened. Some dishes, windows, etc., broken; a few instances of cracked plaster; unstable objects overturned. Disturbances of trees, poles, and other tall objects sometimes noticed. Pendulum clocks may stop. (V to VI Rossi-Forel scale.) | XI. Few, if any, (masonry) structures remain standing. Bridges destroyed. Broad fissures in ground. Underground pipelines completely out of service. Earth slumps and land slips in soft ground. Rails bent greatly. |
| VI. Felt by all, many frightened and run outdoors. Some heavy furniture moved; a few instances of fallen plaster or damaged chimneys. Damage slight. (VI to VII Rossi-Forel scale.) | XII. Damage total. Waves seen on ground surfaces. Lines of sight and level distorted. Objects thrown upward into air. |
| VII. Everybody runs outdoors. Damage negligible in buildings of good design and construction; slight to moderate in well-built ordinary structures; considerable in poorly built or badly designed structures; some chimneys broken. Noticed | |

Table 6. Annual Risk Equivalent Intensities at Vandenberg AFB

| Annual Risk | Return Period | Maximum Intensity | | |
|-------------|---------------|-------------------|------------|--------------|
| | | Acceleration | Velocity | Displacement |
| 0.9 | 1.11 | V | IV | III |
| 0.5 | 2 | V - VI | IV - V | IV |
| 0.2 | 5 | VI | V | V |
| 0.1 | 10 | VI | VI | VI |
| 0.05 | 20 | VII | VI | VII |
| 0.02 | 50 | VII | VII | VIII |
| 0.01 | 100 | VII | VII - VIII | VIII |
| 0.005 | 200 | VIII | VIII | IX |
| 0.002 | 500 | VIII | VIII - IX | X |
| 0.001 | 1000 | VIII | IX | X |

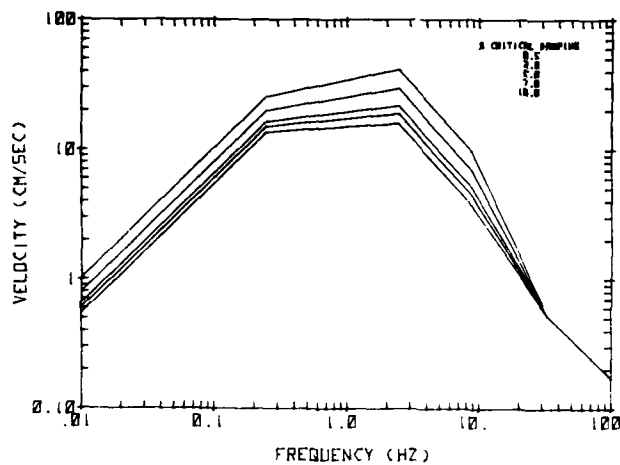
3.5 Composite Design Response Spectra

The spectral characteristics of ground motion are typically represented in the form of response spectra. These spectra represent the maximum response of a simple, viscous-damped harmonic oscillator over a range of natural periods for a specified percentage of critical damping. Methods have been developed to estimate upper limit response spectra given the expected levels of ground motion at the site of interest¹⁹ that are known as design response spectra. Newmark et al²⁰ have developed one set of commonly used amplification factors which are given in Table 7. These values are used to modify the peak ground acceleration and displacement levels estimated for a site to obtain the response spectra levels at the specified frequencies. The levels of critical damping correspond to various foundation soil conditions at the site of interest. The lower values correspond to hard rock with increasing critical damping correlating to decreasing material rigidity.

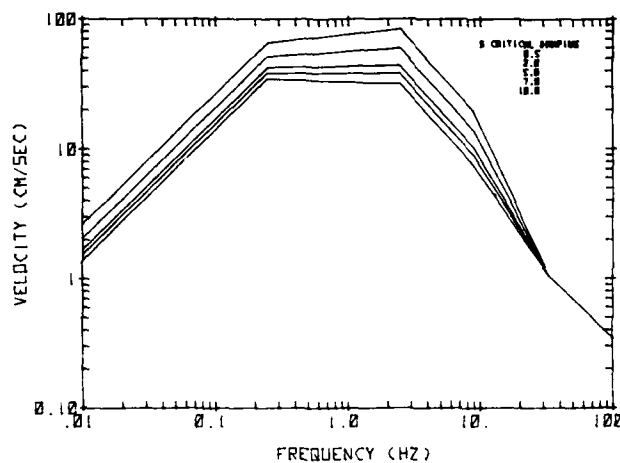
Composite response spectra have been calculated for various risk levels at the Point Arguello site for both the annual and 20-yr lifetime ground motion values. These design spectra are shown in Figures 6a to 6c and 7a to 7c. It should be noted that these response spectra are not likely to represent the design response spectra for any one earthquake. This is because the peak ground motions on which they are based have the same return period but would probably be generated by different earthquakes.⁹ Thus, it may be more accurate to view this representation as the estimated upper limits over frequency bands than over the entire spectra.

19. Hays, W., Algermissen, S., Estinesa, A., Perkins, D., and Rinehart, W., (1975) Guidelines for Developing Design Earthquake Response Spectra, U.S. Geol. Surv. Technical Report M-114.

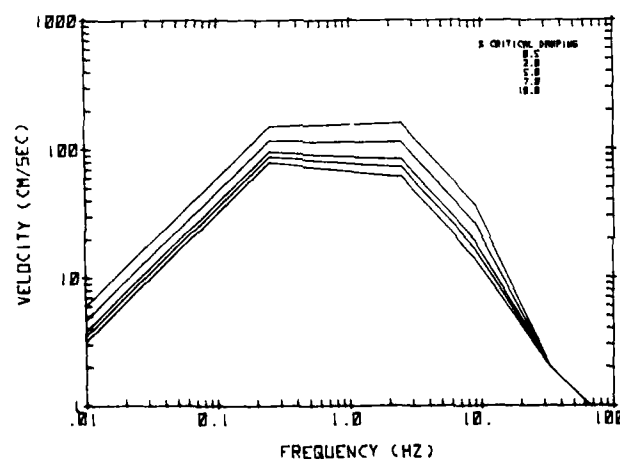
20. Newmark, N., Blume, J., and Kapur, K. (1973) Design response spectra for nuclear power plants, Am. Soc. Civil Eng., Structural Engineering Meeting, San Francisco, CA.



(a)

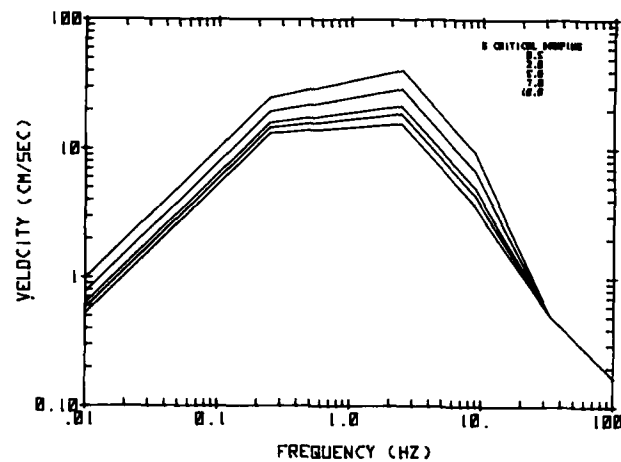


(b)

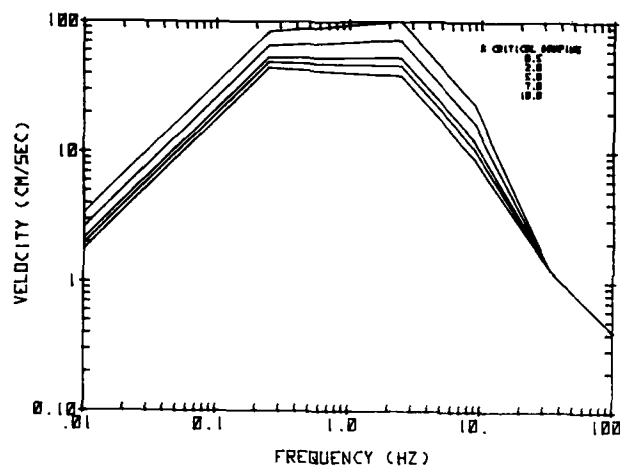


(c)

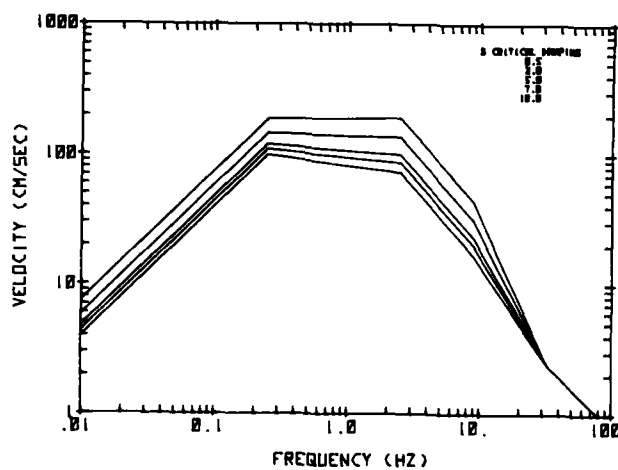
Figure 6. Composite Horizontal Design Response Spectra for Vandenberg AFB Using 10 (a), 100 (b), and 1000 (c) Year Return Period Ground Motions



(a)



(b)



(c)

Figure 7. Twenty-Year Lifetime Composite Horizontal Response Spectra for Vandenberg AFB Using Ground Motions With Risks of 0.9 (a), 0.1 (b), and 0.01 (c)

Table 7. Horizontal Design Response Spectra Amplification Factors

| Critical Damping (%) | Acceleration | | | Displacement (cm) |
|----------------------|--------------|------|--------|-------------------|
| | 33 Hz | 9 Hz | 2.5 Hz | 0.26 Hz |
| 0.5 | 1.0 | 4.96 | 5.95 | 3.20 |
| 2.0 | 1.0 | 3.54 | 4.25 | 2.50 |
| 5.0 | 1.0 | 2.61 | 3.13 | 2.05 |
| 7.0 | 1.0 | 2.27 | 2.72 | 1.88 |
| 10.0 | 1.0 | 1.90 | 2.28 | 1.70 |

4. NON-STATISTICAL HAZARD ANALYSIS

4.1 Geologic Methods

While the statistical approach to seismic hazard analysis has the advantage of including time as one parameter of the estimation process, it has the limitation of the assumption that recent seismic history is indicative of future occurrences. Many large earthquakes have occurred on faults which might be considered innocuous on the basis of recent seismic activity.^{21, 22} One significant example of this limitation was the San Fernando Earthquake of 9 February 1971. In addition, earthquake catalogues for China, Japan, and the Middle East, which cover periods of 2000 to 3000 years, indicate long-term spatial and temporal variations which, if similar variations occurred in the United States, would not be apparent in the short record available; approximately 150 years.^{21, 23, 24} These same studies, however, indicate that knowledge of Quaternary faulting is usually sufficient to detect the causative faults of large earthquakes.

4.2 Quaternary Faulting Near Vandenberg AFB

Examination of fault maps for the Vandenberg AFB region^{25, 26} was conducted and a map was prepared of all known faults within 50 km and all faults with indications of Quaternary displacement within 100 km of Point Arguello (Figure 8). It should be noted that, particularly offshore, the known faults are not considered to be a complete description of the faulting patterns and significant modification would be expected with future investigations. In Figure 8, the heavy lines represent faults or fault systems with known indications of Quaternary movement while the thinner lines are faults lacking such indication. The lack of such indication does not guarantee Quaternary displacements have not taken place. In addition, several inferred

(Due to the large number of references cited above, they will not be listed here. See References, page 31.)

fault extensions have been made² and these are shown in Figure 1. For the purposes of this section, only faults represented in Figure 8 were utilized, however, some discussions of the effects of the inferred fault trends are given below.

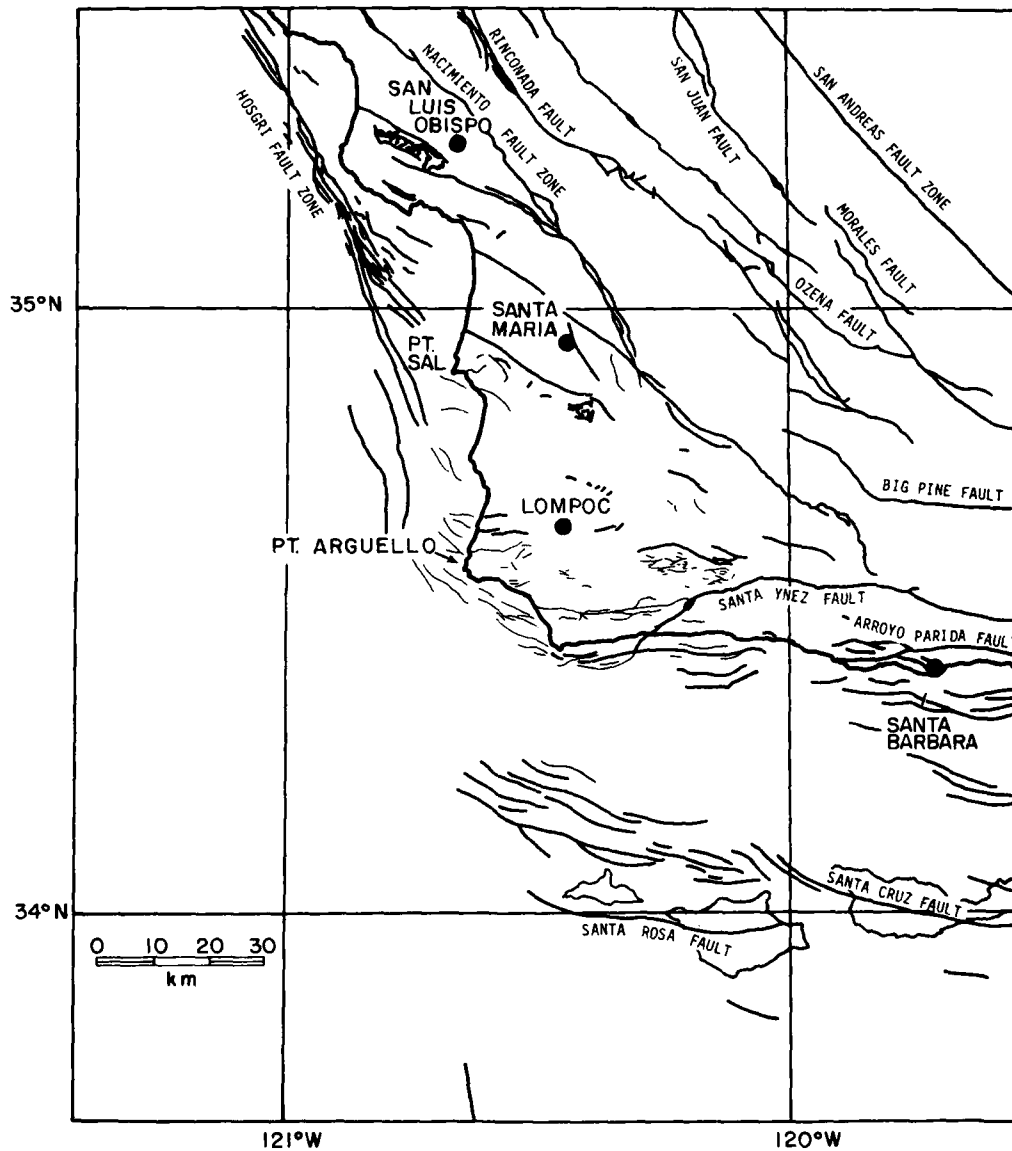


Figure 8. All Faults Within 50 km and Faults With Quaternary Displacements Within 100 km of Point Arguello. Derived from Jennings (1975) and Buchanan-Banks et al (1978). (Heavy trace implies known Quaternary movement)

4.3 Maximum Credible Earthquakes

Given the known faults in the vicinity of Vandenberg AFB, it is possible to estimate the maximum magnitude earthquake that each fault could generate. The procedure is to determine the maximum fault rupture distance, typically between 20 percent and 50 percent of the total fault.²⁷ In any case, the judgement on appropriate fault length is subjective but an error of even a factor of two can be shown to be of minor importance within the accuracies of other steps of the procedure.

Several empirical relationships between fault length and earthquake magnitude have been developed.²⁸ The equation developed by Bonilla²⁹ has been applied to major faults in California by Greensfelder.⁹ This relation is given by

$$M = 5.29 + 1.4 \log L \pm 0.26 \quad (8)$$

where L is the fault length in km and was utilized in this study to calculate maximum credible earthquakes not evaluated by Greensfelder.⁹

The majority of faults near Vandenberg AFB have maximum credible earthquakes of between 6 and 6.5 M_L . However, the maximum ground motion levels are essentially set by a small subset of all the faults. These faults and associated maximum credible earthquakes are given in Table 8. It should be noted that wide variation exists in the empirical data between fault length and maximum magnitude earthquakes. It is very possible that faults not included in this list could support comparable magnitude earthquakes.

4.4 Maximum Credible Ground Motions

Using the maximum credible earthquakes listed in Table 8, contour plots of estimated peak ground acceleration, velocity, and displacement were made for western Santa Barbara County. These maps were constructed under the assumption that the maximum credible earthquake could occur at any point on the fault zone. The ground motion levels were calculated using the ground motion attenuation functions discussed in Section 3.3 at a 90 percent confidence level. No contour was plotted closer than 8 km to the causative fault due to the great uncertainty in ground motion levels close to zones of faulting, and accelerations greater than one g

27. Albee, A., and Smith, J. (1966) Earthquake characteristics and fault activity in Southern California, in Engineering Geology in Southern California, R. Lung and R. Proctor, Editors, Los Angeles section of the Association of Engineering Geologists, pp 9-33.

28. Slemmons, D. (1977) Faults and Earthquake Magnitude, U.S. Army Engineer Waterways Experiment Station, Miscellaneous Paper S-73-1.

29. Bonilla, M. (1970) Surface faulting and related effects, in Earthquake Engineering, R. Wiegel, Editor, Prentice-Hall, pp 47-74.

were not plotted. By virtue of the equations used, these maps are for average soil conditions. The contour maps are displayed in Figures 9a to 9c. As was noted in Section 4.3, smaller faults could generate earthquakes sufficiently large to distort the maximum ground level contours presented in these figures. Predicting such an occurrence is beyond the present capabilities of seismology.

Inspection of Figures 9a to 9c indicate that Point Sal and Point Arguello are at the extremes of maximum credible ground motion estimated for Vandenberg AFB. At Point Sal the ground motion levels are controlled by faulting on the Hosgri Fault Zone while at Point Arguello the determining fault for acceleration and velocity is the Hosgri Fault Zone while the San Andreas determines the maximum displacement. The estimated ground motion levels for the causative earthquakes at each site is given in Table 9.

Table 8. Major Faults Near Vandenberg AFB and Associated Maximum Credible Earthquakes

| Fault | Maximum Credible Earthquake (M_L) |
|-------------------------|--|
| San Andreas Fault Zone | 8.5 |
| Big Pine Fault | 7.5 |
| Santa Ynez Fault | 7.5 |
| Rinconada Fault | 7.5 |
| Hosgri Fault Zone | 7.5 |
| Nacimiento Fault Zone | 7.0 |
| Santa Cruz Island Fault | 6.75 |
| Santa Rosa Island Fault | 6.75 |

Table 9. Maximum Credible Ground Motions at Point Sal and Point Arguello (90% confidence level)

| Motion (Source) | Point Sal | Point Arguello | |
|--|----------------------|----------------------|---------------------------|
| | Hosgri Fault Zone | Hosgri Fault Zone | San Andreas Fault Zone |
| Acceleration (cm/sec ²) | 1288.8 | 678.6 | 387.2 |
| Velocity (cm/sec) | 200.2 | 110.8 | 91.4 |
| Displacement (cm) | 83.8 | 54.3 | 64.6 |

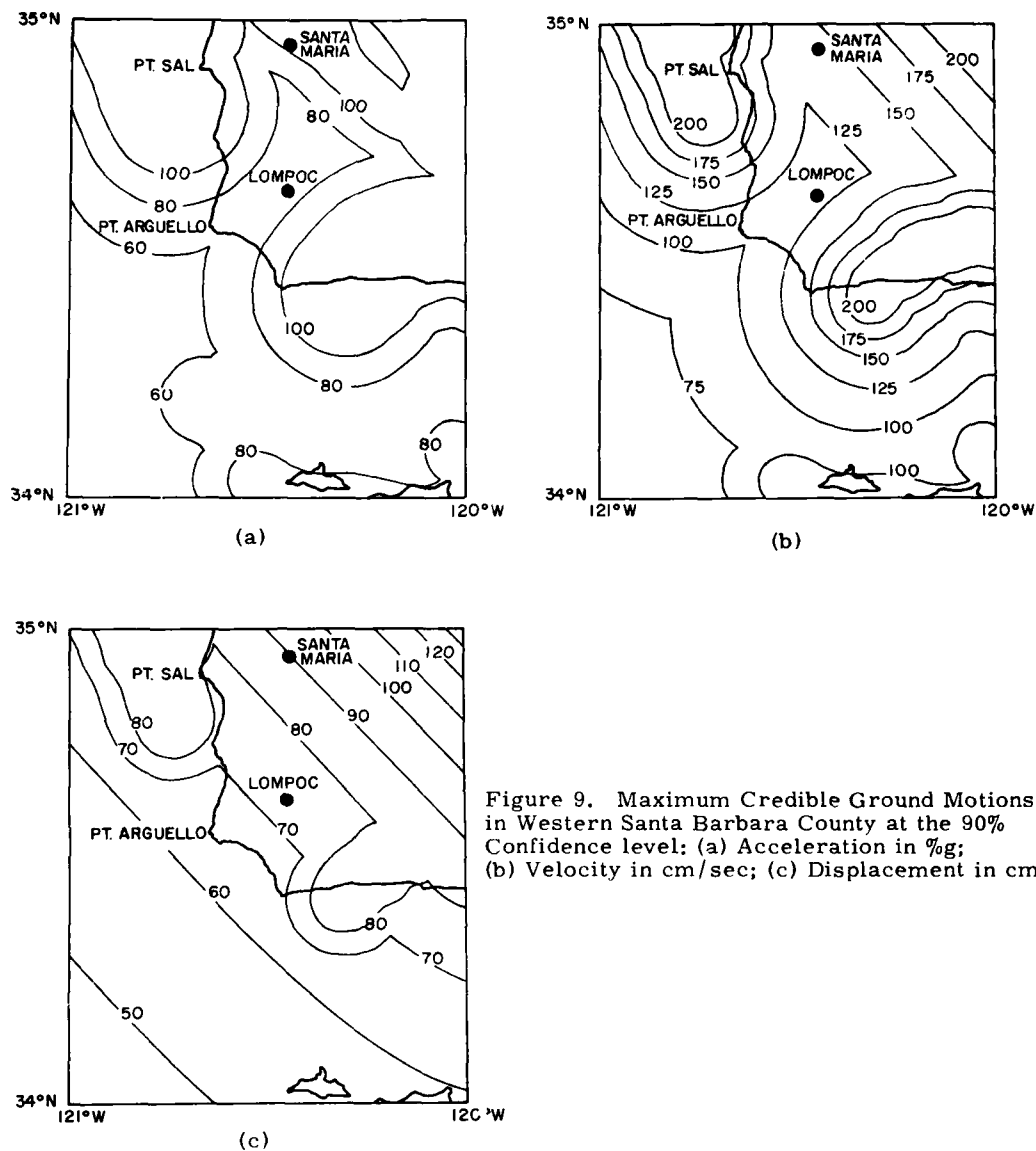
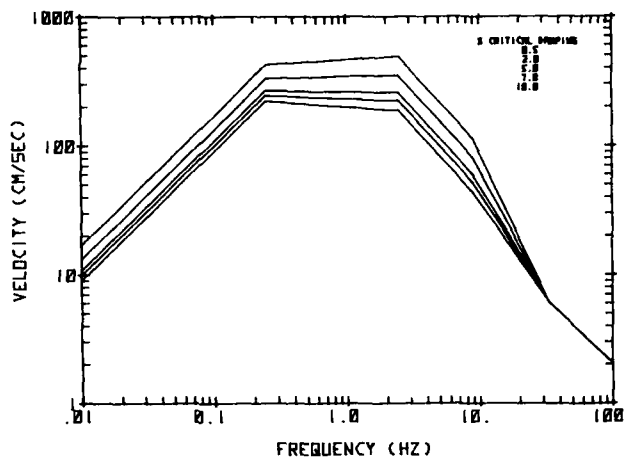


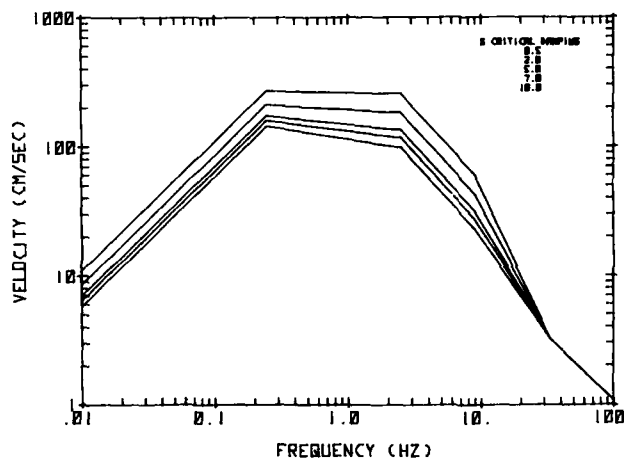
Figure 9. Maximum Credible Ground Motions in Western Santa Barbara County at the 90% Confidence level; (a) Acceleration in %g; (b) Velocity in cm/sec; (c) Displacement in cm

4.5 Maximum Credible Design Response Spectra

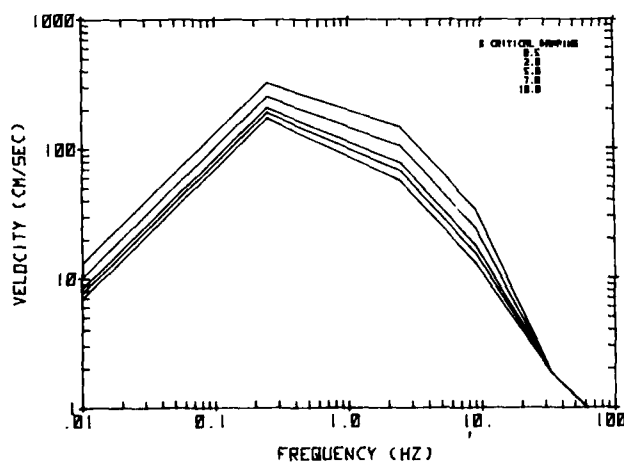
Design response spectra for each of the causative earthquakes in Table 9 were calculated using the methods described in Section 3.5. These spectra are shown in Figures 10a to 10c. In this case, the response spectra are not composite in nature as all ground motions used to generate each display result from one earthquake. The only significant change among the spectra, besides amplitude levels, is the reduced high frequency amplitude for the San Andreas event. This results from greater attenuation at high frequency over a much longer travel path as compared to the Hosgri Fault events.



(a)



(b)



(c)

Figure 10. Maximum Credible Horizontal Design Response Spectra for:
(a) Point Sal; (b) Point Arguello for an Earthquake on the Hosgri Fault Zone;
(c) Point Arguello for an Earthquake on the San Andreas Fault Zone

5. LOCAL EARTHQUAKE HISTORY

The location of earthquakes near Vandenberg AFB is hampered by the lack of local seismographs, the large azimuthal gap in station coverage as a result of the proximity of the Pacific Ocean, and insufficient data for crustal velocity determination.³⁰ For these reasons, the association of seismic activity in the study area with any one, or a set, of faults is impossible. The continuing seismic activity does imply that many of the minor faults within the region present, at least, a local seismic hazard. From 1932 to 1975 the Earthquake Data File reports 135 earthquakes with magnitudes between 2.5 to 4.9 M_L within 50 km of Point Arguello.

In Figure 11, earthquake epicenters in western Santa Barbara County, as reported by Sylvester and Darrow² are shown. An estimate of the level of seismic activity has been made by Battis⁵ for the Coastal Faults Source Region, as shown in Figure 2, that includes the Vandenberg AFB region. The cumulative recurrence curve for this region is displayed in Figure 12. The recurrence function fit to this data is given by

$$\text{Log}(N) = 4.37 - 1.21 m_b \quad (9)$$

where N is the number of events per year per 1000 km^2 of magnitude m_b or greater.

Over the period 1928 to 1973, the region under study experienced Modified Mercalli Intensity IV, or greater, on 53 occasions with a maximum intensity of VIII near Point Arguello and VII for the remaining area.³¹ The definition of the Modified Mercalli scale is given in Table 5 with the description of effects associated with these intensity levels. While correlation of peak ground motion amplitude with intensity is poor, Trifunac and Brady¹⁵ have evaluated equations that allows one to estimate the levels of ground motion associated with a given intensity level. These equations predict peak accelerations of 16, 130, and 259 cm/sec^2 , velocities of 2, 13, and 23 cm/sec and displacements of 1.7, 6.3, and 9.8 cm for Modified Mercalli intensities of IV, VII, and VIII respectively.

During recent history, the largest event to effect the Vandenberg AFB region was the 1927 Lompoc earthquake. A maximum Rossi-Forel intensity IX was reported to cover the area of Vandenberg AFB from Purisima Point south and Rossi-Forel intensity VIII in most of western Santa Barbara County (Figure 13).

30. Gawthrop, W. (1975) Seismicity of the Central California Coastal Region, U.S.G.S. Open-File Report 75-134.

31. Braze, R. (1976) An Analysis of Earthquake Intensities With Respect to Attenuation, Magnitude, and Rate of Recurrence, National Geophysical and Solar-Terrestrial Center, NOAA Technical Memorandum EDS NGSDC-2.

Conversions of Rossi-Forel to Modified Mercalli intensity are given in Table 5. The epicenter of this event has not been conclusively located but would appear to lie on an offshore fault to the west of Point Arguello.^{32, 33} The reported magnitude of this event was 7.3 M_L . In Figure 13, the various suggested epicenters of the event, as reported by Hanks³³ are shown.

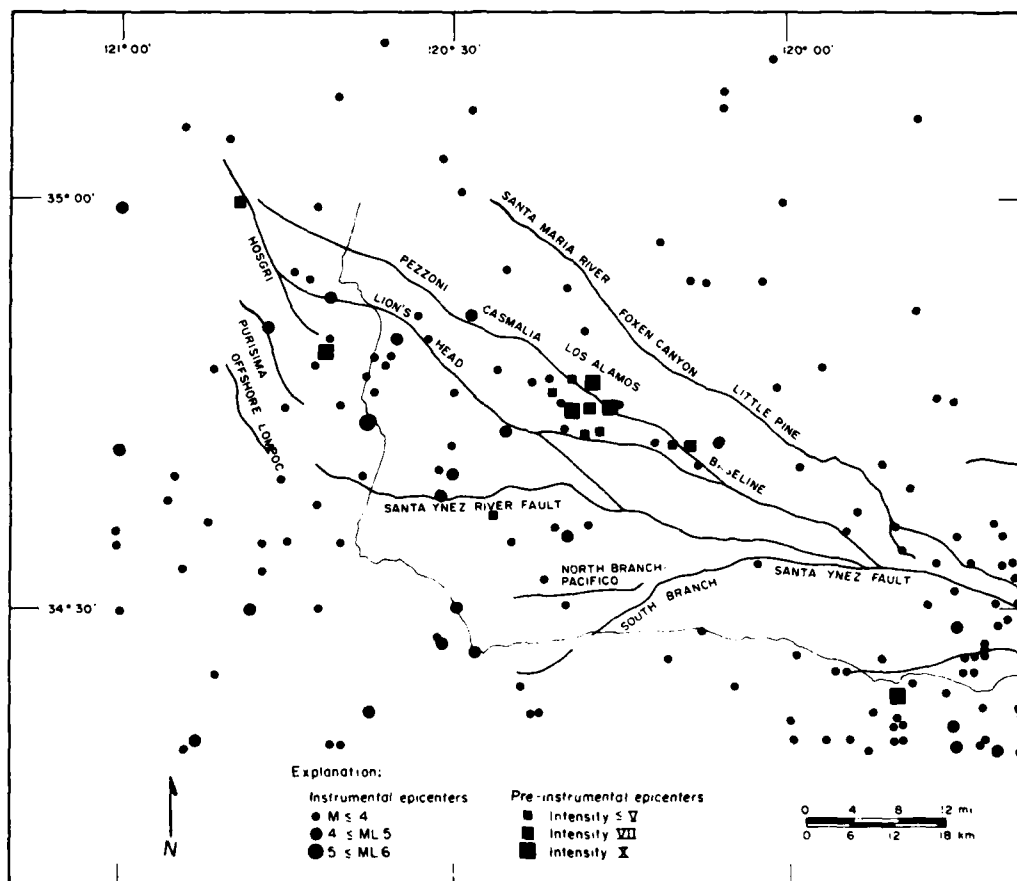


Figure 11. Earthquake Epicenters, Western Santa Barbara County, California. Compiled from Townely and Allen (1939), Coffman and Hake (1973), California Institute of Technology (1977) (from Sylvester and Darrow, 1979)

32. Gawthrop, W. (1978) The 1927 Lompoc, California earthquake, Bull. Seism. Soc. Am. 68:1705-1716.
33. Hanks, T. (1979) The Lompoc, California earthquake (November 4, 1927; $M = 7.3$) and its aftershocks, Bull. Seism. Soc. Am. 69:451-462.

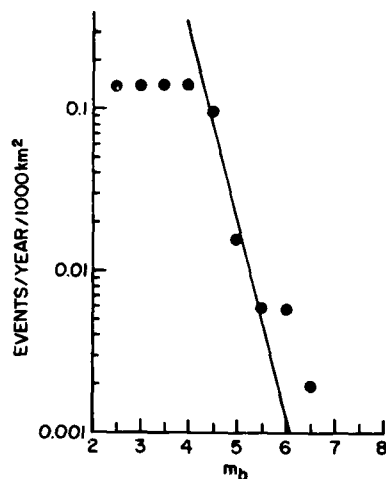


Figure 12. Cumulative Recurrence Curve for the Coastal Faults Source Region

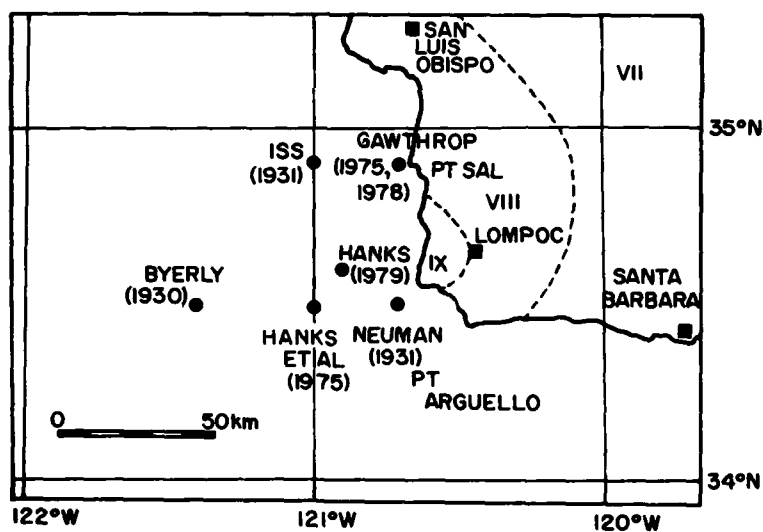


Figure 13. Epicenter Determinations for the 1927 Lompoc Earthquake With Rossi-Forel Iseismal Contours (after Hanks, 1979)

6. CONCLUSIONS

A seismic hazards analysis was conducted for western Santa Barbara County, California, including Vandenberg AFB. Probabilistic estimates of seismic risk for this region suggest that the facility should experience Modified Mercalli Intensity V somewhat less than once a year, which is in good agreement with actual experience during the period 1928 to 1978. Deterministic estimates of the seismic hazard, based on maximum credible earthquakes for faults near the installation, were also made. Extrapolation of the probabilistic risk curves to much lower levels than those actually calculated, appear to be in agreement with the deterministic results.

Historically, the largest event to affect the region appears to have been the 1927 Lompoc earthquake that resulted in approximately Modified Mercalli Intensity IX, in the area between Point Arguello and Purisima Point. Poor instrumental coverage at the time of the earthquake makes the association of this event with any particular fault system impossible.

References

1. Crouch, J. (1979) Neogene tectonic evolution of the California continental borderland and western transverse ranges, Geol. Soc. Am. Bull. 90:338-345.
2. Sylvester, A., and Darrow, A. (1979) Structure and neotectonics of the Western Santa Ynez fault system in Southern California, Tectonophysics 52:389-405.
3. Hsü, K. (1971) Franciscan melanges as a model for eugeosynclinal sedimentation and underthrusting tectonics, J. Geophys. Res. 76:1162-1170.
4. Atwater, T. (1970) Implications of plate tectonics for the Cenozoic tectonic evolution of Western North America, Geol. Soc. Am. Bull. 81:3515-3536.
5. Johnson, J., and Normark, W. (1974) Neogene tectonic evolution of the Salinian block, West-Central California, Geology 2:11-14.
6. Battis, J. (1978b) Geophysical Studies for Missile Basing: Seismic Risk Studies in the Western United States, Texas Instruments Inc., Final Scientific Report ALEX(02)-FSR-78-01.
7. Meyers, H., and von Hake, C. (1976) Earthquake Data File Summary, National Geophysical and Solar-Terrestrial Data Center Report KGRD-5.
8. Richter, C. (1958) Elementary Seismology, W. H. Freeman and Co., San Francisco, CA.
9. Greensfelder, R. (1974) Maximum Credible Rock Acceleration From Earthquakes in California, California Division of Mines and Geology, Map Sheet 25.
10. Battis, J. (1978a) Geophysical Studies for Missile Basing Seismic Risk Studies in the Western United States, Texas Instruments Inc., Scientific Report No. 2, ALEX(02)-ISR-78-01.
11. Esteve, L. (1970) Seismic risk and seismic design decisions, in Seismic Design for Nuclear Power Plants, R. Hansen, Editor, MIT Press, pp 142-182.
12. McGuire, R. (1974) Seismic Structural Response Risk Analysis Incorporating Peak Response Regressions on Earthquake Magnitude and Distance, M.I.T. Dept. of Civil Eng. Research Report R74-51.
13. Cornell, C. (1968) Engineering seismic risk analysis, Bull. Seism. Soc. Am. 58:1503-1606.
14. McGuire, R. (1976) FORTRAN Computer Program for Seismic Risk Analysis, U.S. Geol. Surv. Open-File Report 76-67.
15. Allen, C., St. Amund, P., Richter, C., and Nordquist, J. (1965) Relationship between seismicity and geological structure in the Southern California Region, Bull. Seism. Soc. Am. 55:753-797.

References

16. Trifunac, M., and Brady, A. (1975) On the correlation of seismic intensity scales with peaks of recorded strong ground motion, Bull. Seism. Soc. Am. 65:139-162.
17. McGuire, R. (1977) The use of intensity data in seismic-hazard analysis, Proc. Sixth World Conf. on Earthquake Engineering, pp 709-714.
18. Murphy, J., and O'Brien, L. (1977) The correlation of peak ground acceleration amplitude with seismic intensity and other physical parameters, Bull. Seism. Soc. Am. 67:877-915.
19. Hays, W., Algermissen, S., Estinesa, A., Perkins, D., and Rinehart, W. (1975) Guidelines for Developing Design Earthquake Response Spectra, U.S. Geol. Surv. Technical Report M-114.
20. Newmark, N., Blume, J., and Kapur, K. (1973) Design response spectra for nuclear power plants, Am. Soc. Civil Eng., Structural Engineering Meeting, San Francisco, CA.
21. Allen, C. (1975) Geologic criteria for evaluating seismicity, Geol. Soc. Am. Bull. 86:1041-1057.
22. Sykes, L. (1971) Aftershock zones of great earthquakes, seismicity gaps and earthquake prediction for Alaska and the Aleutians, J. Geophys. Res. 76:8021-8041.
23. McGuire, R. (1979) Adequacy of simple probability models for calculating felt-shaking hazard, using the Chinese earthquake catalog, Bull. Seism. Soc. Am. 69:877-892.
24. York, J., Cardwell, R., and Ni, J. (1976) Seismicity and quaternary faulting in China, Bull. Seism. Soc. Am. 66:1983-2002.
25. Jennings, C. (1975) Fault Map of California, California Division of Mines and Geology, Geologic Data Sheet 1.
26. Buchanan-Banks, J., Pampeyan, E., Wagner, H., and McCulloch, D. (1978) Preliminary Map Showing Recency of Faulting in Coastal South-Central California, U.S. Geol. Surv. Map MF-910.
27. Albee, A., and Smith, J. (1966) Earthquake characteristics and fault activity in Southern California, in Engineering Geology in Southern California, R. Lung and R. Proctor, Editors, Los Angeles section of the Association of Engineering Geologists, pp 9-33.
28. Slemmons, D. (1977) Faults and Earthquake Magnitude, U.S. Army Engineer Waterways Experiment Station, Miscellaneous Paper S-73-1.
29. Bonilla, M. (1970) Surface faulting and related effects, in Earthquake Engineering, R. Wiegel, Editor, Prentice-Hall, pp 47-74.
30. Gawthrop, W. (1975) Seismicity of the Central California Coastal Region, U.S.G.S. Open-File Report 75-134.
31. Braze, R. (1976) An Analysis of Earthquake Intensities With Respect to Attenuation, Magnitude, and Rate of Recurrence, National Geophysical and Solar-Terrestrial Center, NOAA Technical Memorandum EDS NGSDC-2.
32. Gawthrop, W. (1978) The 1927 Lompoc, California earthquake, Bull. Seism. Soc. Am. 68:1705-1716.
33. Hanks, T. (1979) The Lompoc, California earthquake (November 4, 1927; M = 7.3) and its aftershocks, Bull. Seism. Soc. Am. 69:451-462.